ELSEVIER

Journal of Photochemistry and Photobiology A: Chemistry 128 (1999) 47–55

Journal of Photochemistry and Photobiology A:Chemistry

www.elsevier.nl/locate/jphotochem

Comparative time-resolved photoconductivity and absorption spectroscopy studies on dark secondary reactions following the photoreduction of benzophenone by triethylamine

M. Dossot, X. Allonas, P. Jacques *

Département de Photochimie Générale, UMR CNRS No. 7525, Ecole Nationale Supérieure de Chimie de Mulhouse, 3, rue Alfred Werner, F-68093 Mulhouse Cedex, France

Received 7 July 1999; accepted 12 July 1999

Abstract

The dark secondary reactions following the photoreduction of benzophenone by triethylamine constitute an example of tricky reactions involving radicals throughout proton, hydrogen atom and electron transfer. In this work, nanosecond transient absorption spectroscopy is used to detect the influence of hydrogen bonding ability of the solvent on these reactions by means of adding water or methanol to acetonitrile solutions. The effect of increasing polarity is studied with the addition of $LiClO_4$ and it is found at this occasion that dark processes are also sensitive to Lewis acid-base properties of the solvent. The secondary reactions in the reference medium, i.e., neat acetonitrile, are conveniently monitored by photoconductivity technique, which reveals to be a useful complement to absorption spectroscopy and underlines the crucial role of residual water on the reactions. ©1999 Elsevier Science S.A. All rights reserved.

Keywords: Benzophenone; Photoreduction; Salt effect; Photoconductivity; Transient absorption

1. Introduction

Picosecond and nanosecond flash photolysis experiments have clearly evidenced that the photoreduction of benzophenone (BP) by tertiary aromatic amines in polar solvents occurs by a two-step mechanism [1–6]. First an electron is transferred from the amine to the benzophenone triplet state (^{3}BP), leading to an encountered triplet ion pair (IP). This step is next followed by a fast proton transfer within the geminate IP to form ketyl ($BPH^\bullet$) and aminyl radicals. The IP in acetonitrile (ACN) shows a broad absorption band centred around 620–660 nm and its lifetime is around 100–300 ps, according to the amine used [1–6]. In the case of tertiary aliphatic amines, the photoreduction of BP is thought to follow the same process, as shown in Eq. (1). However, the situation differs by the shorter lifetime of the intermediate IP. The detection at 610–620 nm of its transient absorption band has been achieved by picosecond flash photolysis in the photoreduction of BP by triethylamine (TEA) in ACN and methanol (MeOH) [5,7]. Contrary to aromatic amines, the lifetime of the IP is estimated to be about 15 ps, and the challenge to detect it prevents to follow precisely its kinetic [5,7]. The proton transfer step is, thus, concluded to be very fast and to occur within a contact ion pair (CIP) when the tertiary amine is aliphatic. Besides, in ACN the ketyl radical quantum yield Φ_{RAD} is almost 1 with BP/TEA [8], whereas it falls to 0.2 with BP/diethylaniline [5]. In nanosecond transient absorption (NTA) spectroscopy, no primary ion species has been detected in ACN solutions, confirming the ultra-fast proton transfer within the CIP [5,9].

An other important specificity of TEA is that dark secondary reactions take place after the primary photoreduction process [5,8–12]. Indeed, a slow absorption growth around 625 nm, due to the ketyl anion ($BP^{\bullet -}$), has been observed in some liquid media. In neat MeOH, the rise-time is in the microsecond time-scale [5]. In a mixture of ACN/H_2O (v : v 9 : 1) and NaOH 0.02 M, the absorption growth is also observed, but the process follows two kinetics: a fast one produces ketyl anions in several hundreds of nanoseconds and a slowest one in several microseconds [9]. The fast secondary reaction is attributed to the ketyl radical deprotonation by TEA (Eq. (2)) and the slow process to the reduction of the ground state BP by the α-aminoalkyl radical $TEA_{-H}^\bullet$, which may occur either by a hydrogen atom transfer (Eq. (3)) or by an electron transfer (Eq. (4)), depending on the acid-base

---

* Corresponding author. Tel.: +33-3-89-336828; fax: +33-3-89-336895
E-mail address: p.jacques@univ-mulhouse.fr (P. Jacques)

PII: S1010-6030(99)00149-5

properties of the solvent used [5,8–12]. In neat MeOH, the kinetics of the ketyl deprotonation and the BP secondary reduction can not be resolved [5], whereas in the alkaline mixture of ACN/H_2O the kinetics are clearly distinct [9]. It should be noticed that even in the alkaline medium the primary photoreduction gives ketyl radicals and not ions, giving an idea of the strong efficiency of the proton transfer within the CIP [9].

$$ {}^3BP + TEA \xrightarrow{k_{et}} \underset{CIP}{[BP^{\bullet -}TEA^{\bullet +}]} \xrightarrow{k_H} BPH^{\bullet} + TEA_{-H}{}^{\bullet} \quad (1)$$

$$ BPH^{\bullet} + TEA \xrightarrow{k_{dep}} BP^{\bullet -} + TEAH^{+} \quad (2)$$

$$ BP + TEA_{-H}{}^{\bullet} \xrightarrow{k_{red}^{H}} BPH^{\bullet} + TEA_{-2H} \quad (3)$$

$$ BP + TEA_{-H}{}^{\bullet} \xrightarrow{k_{red}} BP^{\bullet -} + TEA_{-H}^{+} \quad (4)$$

The observation of secondary reactions by NTA spectroscopy in neat MeOH or in alkaline ACN/H_2O mixtures, but not in neat ACN [5], seems to indicate that MeOH or H_2O may contribute significantly to the secondary processes, possibly by forming hydrogen bondings. Their role is however not clear, especially concerning the deprotonation of $BPH^{\bullet}$ [9]. It is rather surprising that no secondary reaction is observed in neat ACN. It may be due to a low reaction quantum yield which may prevent the optical detection of species having low extinction coefficient [13]. Since reactions 2 and 4 produce ketyl ions, nanosecond transient photoconductivity offers an interesting alternative to examine the processes in neat ACN by monitoring specifically *free ions*.

In this work, NTA experiments were first conducted to examine the influence of protic solvents by adding amounts of H_2O and MeOH in ACN solutions of BP and TEA. In order to study the effect of increasing medium polarity, addition of $LiClO_4$ was also used. Then, in neat ACN, the photoreduction of BP by TEA was studied by photoconductivity. This technique enables to detect even a small amount of free ions, and among others those eventually coming from the direct separation of the primary CIP.

2. Experimental

2.1. Chemicals

TEA, BP, benzhydrol, diaza-bicyclo[2,2,2]-octane (DABCO) and $LiClO_4$ come from Fluka at the best purity available. Benzophenone and benzhydrol were recrystallised in ethanol and sublimated once before use. DABCO was sublimated and kept under dry argon at 4°C before each use to avoid water adsorption. TEA was freshly distilled under nitrogen. $LiClO_4$ was used as received. ACN and MeOH, from Fluka spectrochemical grade, were used without further purification. Water was twice distilled.

2.2. Time-resolved measurements

Nanosecond transient absorption spectroscopy has been described previously [14]. For the measurement of transient photocurrents, a quartz sample cell with two parallel platinum plates (8 mm × 10 mm) separated by 8 mm was used. In order to avoid saturation effects and to have a spatial homogeneity of the excitation laser beam, this latter was extended by a galilean beam expander (4×). An optical slit shape (3 mm × 5 mm) before the cell selects a homogeneous 15 mm^2 spot. The spot is separated from the electrodes by more than 2 mm to prevent photoreaction at the platinum plates. An electrode bias of 500 V is applied by a power supply to the platinum plates during the acquisition of a signal, and stopped just after it to hinder electrolysis. The transient voltage signal across a 220 Ω resistor is directly fed into a numerical digitizer Tektronik DSA601. In these conditions, the rise-time is ca. 80 ns. The Nd : YAG laser (Continuum Surelite) gives a pulse of 9 ns and 30 mJ at 355 nm and its energy is lower to 1 mJ by using chemical filters. The low energy prevents non-linear phenomena such as photoionisation or triplet–triplet annihilation. The solution (15 ml) is slowly flowed through the cell (which contains 3 ml) during the measurements and the signals are recorded in single shot mode to minimise the consequences of photobleaching. It is degassed by bubbling dry argon for 15 min. The argon flow is kept during the experiment.

3. Results and discussion

3.1. Nanosecond transient absorption spectroscopy

3.1.1. Influence of water and methanol

The photoreduction of BP by TEA was studied in ACN containing variable amounts of H_2O and MeOH. Fig. 1a reports the well known absorption of $BPH^{\bullet}$ centred at 540 nm in neat ACN [3] due to reaction 1. No ion formation is observed in neat ACN (see further, the lower kinetic trace in Fig. 4b) for concentrations of TEA up to 1 M. A different

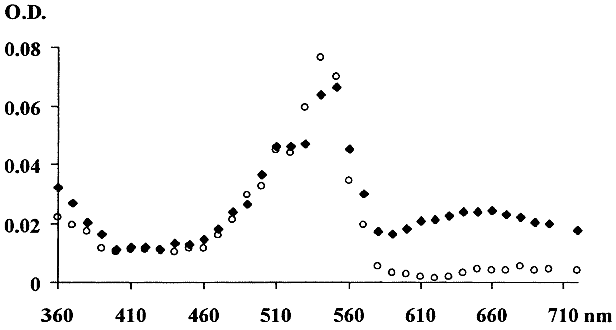

Fig. 1. Transient absorption spectra taken 8 μs after laser pulse of an acetonitrile solution of BP 0.005 M and TEA 0.02 M. (a) (°) neat acetonitrile (b) (◆) addition of 1.8 M of H_2O.

behaviour is observed when protic co-solvents are added to ACN. Fig. 1b shows the influence of H_2O on the transient spectrum of 5 mM of BP and 20 mM of TEA. A broad absorption band centred around 650 nm appears and can be attributed to $BP^{\bullet -}$ involved in hydrogen bondings with a protic medium [1–7,11]. To follow the kinetic of $BP^{\bullet -}$ requires to be aware of the overlap of absorption bands, a problem inherent to the transient absorption technique. It has been shown that ^3BP presents a residual absorption beyond 600 nm in neat ACN [15]. However, in our working conditions, [TEA] is always more than 10^{-2} M and the triplet lifetime is found to be under 40 ns. The triplet gives, thus, a fast transient absorption at the beginning of the signal, whose high depends on the co-solvent mixed with ACN. Consequently, the kinetic traces have been fitted by starting the fit 200 ns after the laser pulse to avoid the triplet contribution. An other problem is the residual absorption of $BPH^{\bullet}$ noticed in Fig. 1a beyond 620 nm. Since the recombination of $BP^{\bullet -}$ takes place over several tens of microseconds, this residual absorption must be minimised to follow the kinetic of ions. That is why a compromise was found by working at 620 nm in ACN/H_2O or ACN/MeOH mixtures. When experiments have been conducted in neat ACN, the eventual absorption of $BP^{\bullet -}$was monitored between 650 and 720 nm, according to the literature data on $BP^{\bullet -}$ in this solvent [1–6,16–18]. Fig. 2 gives an illustration of the kinetic at 620 nm of a solution of 5 mM BP and 20 mM TEA added by H_2O or MeOH. In both cases, following the fast contribution of ^3BP [15], the creation of $BP^{\bullet -}$ occurs with a rise-time of 0.4–1 μs, depending on the working conditions. The kinetic of $BP^{\bullet -}$ formation does not follow a clean first order law. Nevertheless, the collected signals in NTA spectroscopy have all been fitted by a pseudo-first order kinetic in order to compare the different experiments, keeping in mind that this procedure can not reflect the exact behaviour of the system, especially if both reactions 2 and 4 are superposed to each other.

Table 1 collects the pseudo-first order rate constants k_i^{620} obtained at 620 nm by addition of H_2O and MeOH in ACN solutions of BP and TEA. The plots of k_i^{620} versus [H_2O], [MeOH] or [TEA] are not linear and reveal that the formation of $BP^{\bullet -}$ is more complicated than expected from Eqs. (2), (3) and (4). The same conclusions were found in alkaline ACN/H_2O mixtures for the ketyl radical deprotonation [9]. A global trend is the enhancement of k_i^{620} with increasing H_2O or MeOH contents. It should be noted that NTA experiments require important amounts of protic species to observe the formation of $BP^{\bullet -}$. Moreover, our results indicate that alkaline conditions are not necessarily requested to observe the secondary formation of $BP^{\bullet -}$ in ACN.

The increase of k_i^{620} with [TEA] is certainly qualitatively linked to Eq. (2). However, as noted above, TEA alone is not able to bring about secondary processes in neat ACN with a sufficient yield to allow optical detection. It results that H_2O or MeOH should contribute to the deprotonation of $BPH^{\bullet}$ and enhance the quantum yield of the reaction, since the detection becomes feasible in NTA experiments by adding these co-solvents. This contribution is possibly linked to the formation of hydrogen bonding complexes between the protic co-solvent and $BPH^{\bullet}$ or TEA. Such complexes have been observed between TEA and MeOH in the gas, liquid and supercritical states [19]. Moreover, hydrogen bonding complexes are able to stabilise some transient species and strongly influence the reaction mechanism by decreasing the

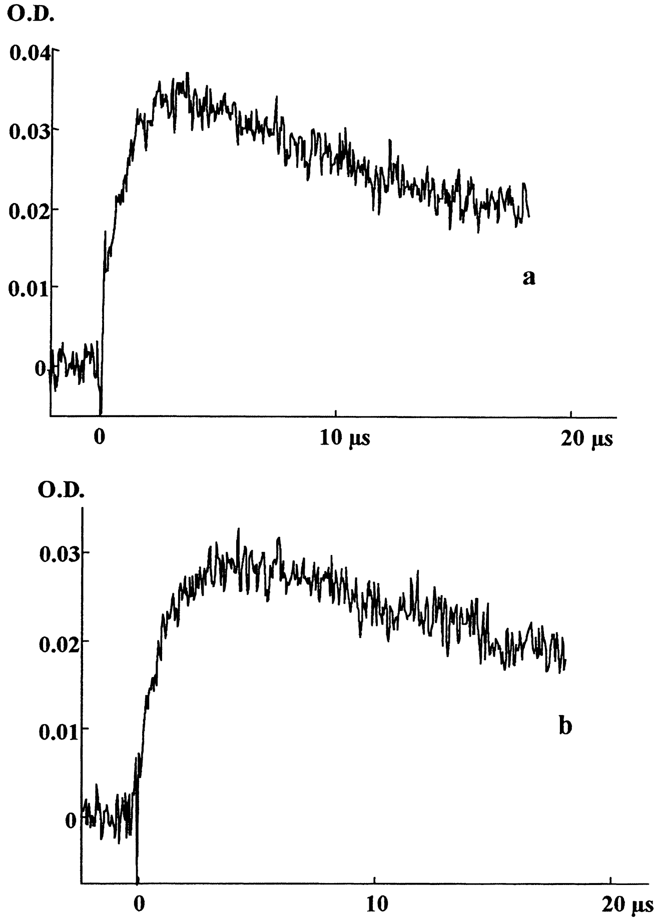

Fig. 2. Transient absorption kinetic traces monitored at 620 nm of an acetonitrile solution of BP 0.005 M, TEA 0.02 M and (a) H_2O 1 M (b) MeOH 2 M.

Table 1
Transient absorption monitoring of the influence of H_2O and MeOH on the first order rate constant k_i^{620} used to fit the secondary ion formation at 620 nm. Solvent is acetonitrile. Concentrations are given in mol l^{-1}. Experimental errors on k_i^{620}, are ± 10%

[BP]	[TEA]	[H_2O]	$k_i^{620} \times 10^{-6}\,s^{-1}$
0.005	0.020	0.5	1.80
0.005	0.020	1.8	3.30
0.005	0.020	4	3.80
		[MeOH]	
0.005	0.020	0.8	0.91
0.005	0.020	1.6	1.10
0.005	0.020	4.1	1.30
0.005	0.040	4.1	1.60
0.005	0.080	4.1	3.00

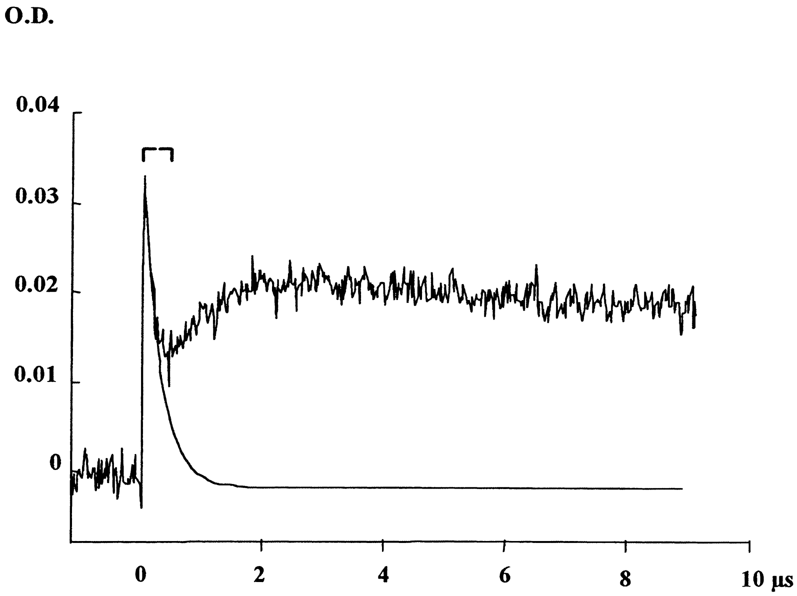

Fig. 3. A transient absorption kinetic trace monitored at 620 nm of a methanol solution of BP 0.005 M and benzhydrol 0.15 M. Solid line shows the decay of ^{3}BP absorption. It is calculated from the triplet lifetime determined by fitting the part of the experimental curve indicated with brackets.

bond strength involved within the complex. For instance, the quenching process of ^{3}BP by N,N-dimethylaminonaphtalene is spectacularly shifted from triplet energy transfer in neat ACN to an electron transfer in MeOH or in ACN/H_2O mixtures [20].

To verify the influence of MeOH on $BPH^\bullet$, solutions of 5×10^{-3} M of BP were added with 0.15 M of benzhydrol (BPOH). It aimed to create ketyl radicals without resorting to TEA. Indeed, ^{3}BP abstracts hydrogen atom from BPOH and produces $BPH^\bullet$ with a quantum yield of 2 [8]. The solvents were neat ACN for a reference solution, ACN with 4 M of MeOH, and neat MeOH. In neat ACN, no ion was observed beyond 620 nm, and the recombination of $BPH^\bullet$ monitored at 540 nm followed a clean second order kinetic. Addition of 4 M of MeOH had no obvious effect on $BPH^\bullet$ and no ion was detected. In neat MeOH, the recombination of $BPH^\bullet$ was not noticeably affected but small amount of ketyl anion was observed at 620 nm as shown in Fig. 3. The shape of the signal is due to the superposition of the triplet absorption decay [15] with the absorption increase of secondary ions created by reaction 5.

$$BPH^\bullet + MeOH \rightarrow BP^{\bullet-} + MeOH_2{}^+ \quad (5)$$

Indeed, since there is no TEA and since BPOH does not seem to affect the secondary reactions, the only possibility to create ions is the deprotonation of $BPH^\bullet$ by MeOH. To our best knowledge, this reaction has not yet been described in the literature. It contributes to be aware of the chemical reactions which can occur between solvent and solutes, especially if acid-base equilibria are possibly involved.

3.1.2. *Influence of LiClO$_4$*

The results obtained with protic co-solvents lead to suspect an influence of hydrogen bondings on the deprotonation of $BPH^\bullet$. However, the influence could only lie in the increase of the relative dielectric constant from neat ACN to neat MeOH or ACN/H_2O mixtures, which should stabilise the ions formed by secondary reactions. The 'normal salt effect' provides a mean to increase the dielectric constant of the medium without adding a chemical susceptible of forming hydrogen bondings [21–23]. It should be kept in mind that the salt possibly gives rise to ionic exchange with transient ion pair, a phenomenon called 'special salt effect' [21–25]. Fig. 4 illustrates the effect of $LiClO_4$ on the secondary reactions by comparing the NTA kinetic traces monitored at 540 and 620 nm in the presence and without the salt. The kinetic trace at 620 nm unambiguously reveals that $LiClO_4$ induces an important formation of $BP^{\bullet-}$ by secondary reactions. To discriminate the origin of these ions, concentration of ground state BP was changed, and the traces at 620 nm were fitted by a pseudo-first order kinetic towards [BP]. The fits were quite accurate as shown for instance by the residual in Fig. 4b. For 5×10^{-3} M and 10^{-2} M of BP, the rate constants obtained were $1.4 \times 10^8\,M^{-1}\,s^{-1}$ and $1.6 \times 10^8\,M^{-1}s^{-1}$, respectively . These values are equal within experimental errors and are relevant to the literature rate constant of reaction 4 ($1.2 \times 10^8\,M^{-1}\,s^{-1}$) in alkaline ACN/$H_2O$ mixtures [9]. The accuracy of the fits, the linear dependence of the rate constant with [BP] and the comparison with the literature data constitute strong arguments to conclude that $LiClO_4$ induces only the secondary reduction of BP (reactions 3 and 4) and not the ketyl deprotonation (reaction 2). As a result, the salt offers the possibility to markedly select the secondary reduction and, therefore, to easily determine the rate constant for this process in ACN containing $LiClO_4$. The average of our experimental values gives $k_{red} = 1.5 \times 10^8\,M^{-1}\,s^{-1}$.

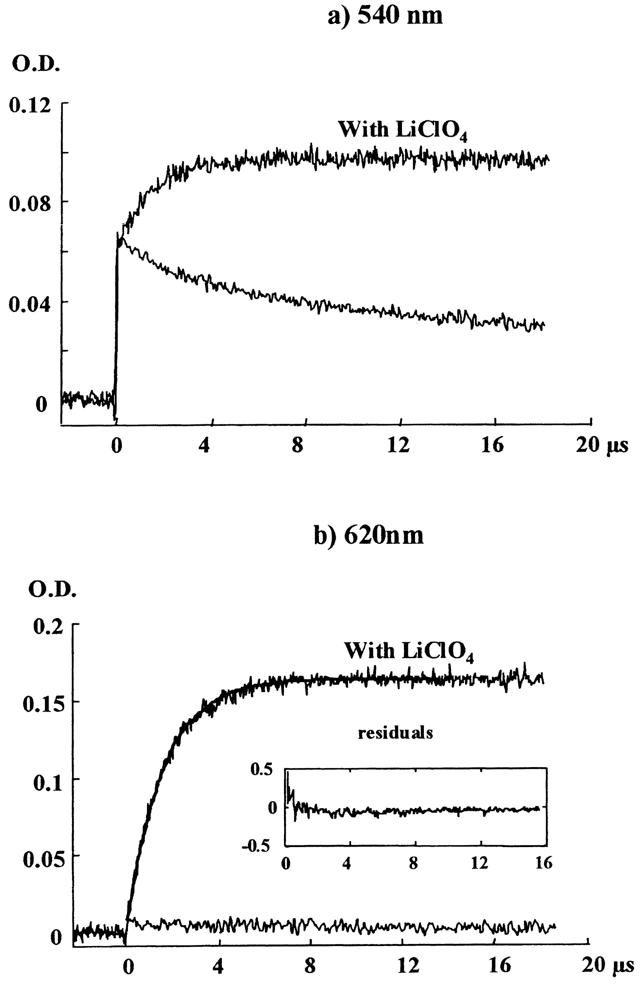

Fig. 4. Transient absorption kinetic traces of an acetonitrile solution of BP 0.005 M and TEA 0.02 M monitored at (a) 540 nm (b) 620 nm in the presence of $LiClO_4$ 0.2 M and without the salt. Inset in (b): residual of the fit of the signal by a first-order kinetic law (solid line).

The shape of the kinetic trace monitored at 540 nm is more complicated than at 620 nm since it is composed by a fast and a slow component. The comparison with the kinetic obtained without adding $LiClO_4$ indicates that the fast component is due to the direct ketyl formation by reaction 1. The slow absorption growth is more doubtful. The fit of this signal by a pseudo-first order kinetic towards [BP] has given same rate constants than at 620 nm within experimental errors. The equality of the kinetics at 540 and 620 nm is consistent with at least two hypothesises: (i) firstly, the slow absorption growth at 540 nm may be due to the same species which gives the absorption trace at 620 nm. In ACN containing $LiClO_4$, the maximum absorption of $BP^{\bullet-}$ shifts from 710 to 620 nm [24] by forming a CIP between the ketyl anion and the lithium cation [24,25]. This ion pair could present a residual absorption at 540 nm, and thus overlap with $BPH^{\bullet}$ (ii) secondly, the slow signal at 540 nm may actually come from the secondary formation of $BPH^{\bullet}$ by reaction 3. In that case, the equality of the rate constants at 540 and 620 nm should imply that reaction 3 and reaction 4 follow the same kinetic. Thus, it should suggest that the hydrogen atom transfer between $TEA_{-H}^{\bullet}$ and BP might occur by an electron transfer followed by a proton transfer, and that the electron transfer should be the limiting step of the secondary reduction. To tentatively discriminate these two hypothesises, the transient spectrum of $BP^{\bullet-}$ in the presence of Li^+ was obtained by quenching ^3BP by DABCO in ACN containing 0.2 M of $LiClO_4$. In neat ACN, the quenching process is an electron transfer which produces efficiently free ions in few nanoseconds [16–18,26,27]. Addition of $LiClO_4$ enables to monitor the formation of the CIP between $BP^{\bullet-}$ and Li^+ [24,25]. The spectra in Fig. 5 clearly show the decrease of ^3BP around 520 nm [1–8] and the concomitant increase of the CIP between $BP^{\bullet-}$ and Li^+ near 610 nm. The spectra c and d seem to indicate that a broad shoulder exists near 550 nm in the absorption band of the CIP. However, the result is not sufficiently accurate to affirm that the slow absorption growth in Fig. 4a is due to $BP^{\bullet-}$ linked with Li^+ (hypothesis i) and not to $BPH^{\bullet}$ (hypothesis ii). At the present time, our results can not definitely discriminate these two explanations.

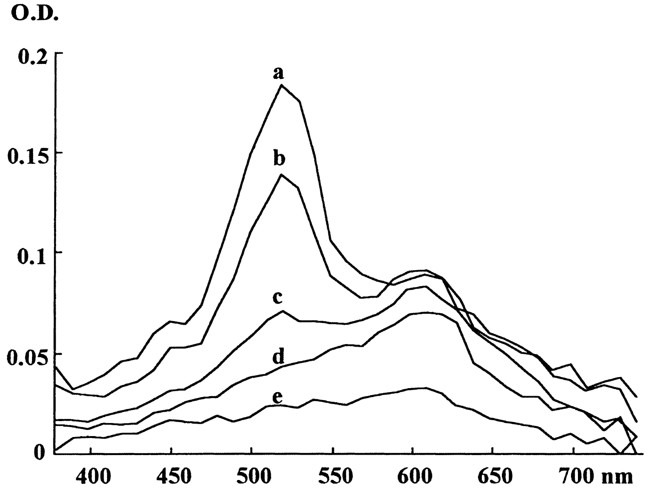

Fig. 5. Time evolution of the spectra of an acetonitrile solution of BP 0.005 M, DABCO 0.02 M and $LiClO_4$ 0.2 M. (a) immediately after pulse, (b) 0.2 µs, (c) 0.4 µs, (d) 2 µs and (e) 10 µs after pulse.

Finally, the influence of the salt concentration has been studied at 620 nm. No obvious dependence of the rate constant with [$LiClO_4$] has been found ranging from 0.05 to 0.6 M. Although the ion quantum yield has not been determined, the relative absorption at 620 nm for the different traces has allowed to notice that the ion yield increased gradually with the salt concentration and levelled off until a concentration of 0.2 M was reached. Regarding the independence of k_{red} and the increase of the ion yield with the concentration of $LiClO_4$, it is reasonable to think that the salt works by changing the solvent properties rather than by a special salt effect. The presence of a hard acid cation like Li^+ brings about the possibility to complex the oxygen atom of BP [22]. Although Raman studies have not evidenced

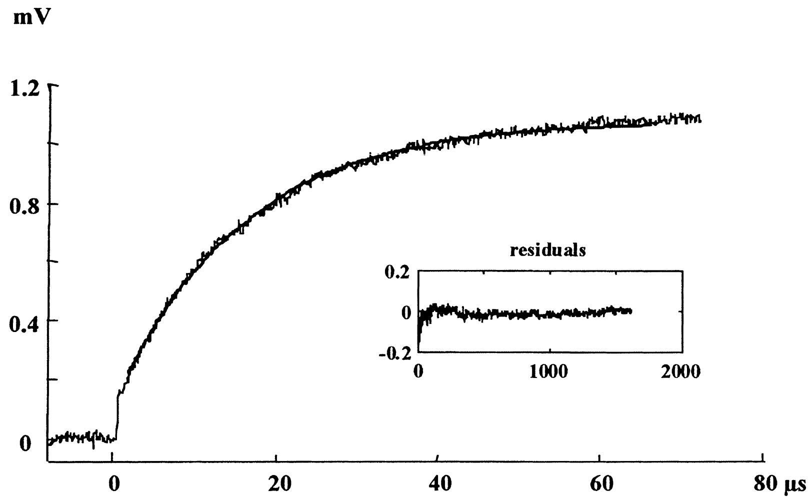

Fig. 6. Photoconductivity signal of an acetonitrile solution of BP 0.005 M and TEA 0.02 M. Inset: residual of the fit by Eq. (6) (solid line).

such a complex between Li^+ and BP in ACN [24], this hypothesis can not be ruled out. Indeed, the stretching mode observed in Raman spectra may not be affected by the complex. The salt is also able to increase the solvent polarity, to change the solvent cage properties [22,23] and to affect the thermodynamics of the reaction by stabilizing the ion pairs [28]. Though it is difficult to determine how $LiClO_4$ is involved in the reaction, the important point is that protic co-solvents are not the only adducts which induce the secondary reduction of BP. Furthermore, it is interesting to note that Li^+ does not affect the primary CIP formed in reaction 1, contrary to the salt effect observed in the quenching of BP by aromatic amines [24,25]. It supports the fast proton transfer within the CIP.

3.2. Nanosecond photoconductivity

The NTA spectroscopy is not sufficiently sensitive to detect secondary reactions in neat ACN. One must add some other chemicals to enhance the quantum yield of these reactions. The most important inconvenient of this method is the change of the solvent properties and the difficulty to determine the influence of the adducts on the rate constants. The nanosecond time-resolved photoconductivity technique offers a good alternative to detect the transient free ions eventually produced by dark secondary reactions in neat ACN. It also avoids the overlap of the absorption bands of the different species involved in the reactions. Besides, the total free ion quantum yield Φ_{ION} is easily determined in comparison with the signal given by the system BP/DABCO in the same conditions of ^3BP formation and quenching. Indeed, as said above, DABCO quenches ^3BP by electron transfer and produces free ions with a quantum yield nearly unity and a fast kinetic [16–18,26,27,29]. In the same working conditions (same pump energy, absorbance and triplet deactivation) the ion quantum yield of the unknown system is given by the ratio of the peak intensities of the photocurrents.

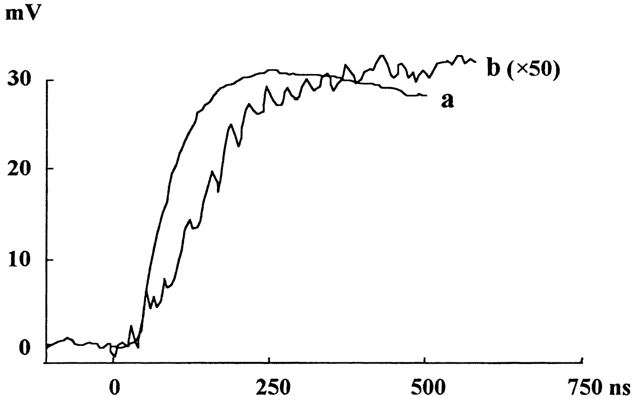

Fig. 7. Comparison on short timescale of the photoconductivity signals of an acetonitrile solution of BP 0.005 M and (a) DABCO 0.02 M (b) TEA 0.02 M.

Fig. 6 shows the signal obtained for 5 mM of BP and 20 mM of TEA at a low energy pulse (2×10^{-6} einstein dm^{-3}). It is quite significant that in the same working conditions the photoconductivity technique leads to a clean, resolved signal contrary to the transient absorption spectroscopy (see the lower trace of Fig. 4b). The shape of the signal reveals two distinct kinetics for ion formation. A submicrosecond rise of photocurrent firstly occurs, leading to an almost vertical trace in Fig. 6 due to the timescale used. It is called ‘fast’ signal, although its rise-time is longer than the time response of the apparatus. A comparison of the shape of the photocurrent given by BP/TEA and BP/DABCO in the submicrosecond timescale (Fig. 7) shows that the slope of the growth is markedly lower in the case of TEA. If the ions come from the primary CIP, the high quenching rate constant of ^3BP by TEA in acetonitrile ($3 \times 10^9\,M^{-1}\,s^{-1}$ [5]) and the short lifetime of the intermediate CIP in the quenching of ^3BP by TEA [5,6] should have given the same curve as with DABCO in our working conditions, i.e., the convolution of the response function of the apparatus with

Table 2
Transient photoconductivity monitoring of the influence of BP, TEA and H_2O on the rate constants of BP secondary reduction (k_{red}), ketyl radical deprotonation (k_{dep}) and Φ_{ION}. Solvent is acetonitrile. Concentrations are in $mol\,l^{-1}$. Experimental errors are ±10% on k_{red} and Φ_{ION}, ±15% on k_{dep}. (a) Maximum residual water in acetonitrile is less than 0.02 M. (b) Addition of 0.05 M of water to the residual one. (c) Calculated with $k_Q = 3 \times 10^9\,M^{-1}\,s^{-1}$ [5] and a triplet lifetime without quencher of 5 μs. (d) Values relative to BP/DABCO with same concentration of BP and same laser intensity than BP/TEA. [DABCO] was always fixed at 0.02 M

[BP]	[TEA]	[H_2O]	$k_Q \times$ [TEA] $10^7\,s^{-1}$ (c)	k_{dep} $10^6\,s^{-1}$	k_{red} $10^6\,s^{-1}$	Φ_{ION} (d)	[TEA]/[BP]
0.006	0.01	(a)	3.0	5.0	1.6	0.07	1.7
0.006	0.02	–	6.0	6.2	1.0	0.09	3.3
0.006	0.03	–	9.0	5.0	1.0	0.14	5.0
0.004	0.02	–	6.0	7.1	5.7	0.13	5.0
0.008	0.02	–	6.0	7.0	1.5	0.1	2.5
0.012	0.02	–	6.0	6.1	2.1	0.06	1.7
0.012	0.02	+0.05 (b)	6.0	8.2	2.6	0.14	1.7

the subnanosecond creation of free ions. It, thus, can be concluded that the first kinetic is due to an other process than the separation of the initial CIP into free ions. Consecutively to the fast process, a ‘slow’ photocurrent appears and produces free ions for several tens of microseconds. The fast signal has been fitted by a first-order kinetic law. A similar procedure was applied to the slow signal but the fast kinetic was taken into account by adding a constant component V_{fast} to the exponential growth of the curve (Eq. (6)).

$$V(t) = V_{slow} \times (1 - e^{-kt}) + V_{fast} \tag{6}$$

This is allowed by the difference on rise-times and the smaller ion quantum yield of the fast process and confirmed by the accuracy of the fit as seen in Fig. 6. In the case of fast signal, the noise of the signal prevented to fit the curve with such accuracy. As a result, this method just gives an estimation of the fast rise of photocurrent. Moreover, the total yield of free ions has been determined, including both the processes 2 and 4. Table 2 collects the data obtained by varying the concentration of BP and TEA. The role of residual H_2O has also been evaluated. The first order rate constants for the slow and the fast components are noted in Table 2 by k_{red} and k_{dep}, respectively (see below). The quenching rates are also indicated in the fourth column to confirm that the primary photoreduction process is not responsible for the fast signal. The shape of the photoconductivity signal in Fig. 6 is close to that found in transient absorption in alkaline ACN/H_2O mixtures [9]. It is, thus, tempting to attribute the fast component to reaction 2 and the slow one to reaction 4. The fast component shows a complex behaviour, since the evolution of k_{dep} with [TEA] or [BP] is not clear. The average value of k_{dep} is ca. $6.1 \times 10^6\,s^{-1}$ in neat ACN and is rather smaller than the value obtained in ACN/H_2O mixtures ($8.3 \times 10^6\,s^{-1}$ [9]). However, addition of 0.05 M of H_2O increases k_{dep} to a very similar value of $8.2 \times 10^6\,s^{-1}$. These results enable us to think that the fast kinetic in photoconductivity signals can be attributed to the deprotonation of the ketyl radical by TEA (reaction 2). Furthermore, Table 2 shows that the rate constant of the slow process is essentially independent of [TEA], but clearly depends on [BP]. Fig. 8 plots the values of k_{red} towards [BP]. A good linear correlation is obtained and leads to a slope of $2 \times 10^8\,M^{-1}\,s^{-1}$ with a correlation coefficient of 0.989. It is in good agreement with the value found for the slow kinetic in alkaline mixtures of ACN/H_2O ($k_{red} = 1.2 \times 10^8\,M^{-1}\,s^{-1}$) by transient absorption experiments [9], even though our value for k_{red} is slightly higher. In transient absorption experiment, large amount of H_2O is required to see the secondary reduction (more than 1 M) whereas the photoconductivity technique needs much lower amount (0.05 M). The change of viscosity is thus marked in the first case, and negligible in the latter. That could be a possible explanation for the little increase of k_{red} in neat ACN compared to alkaline ACN/H_2O mixtures [9]. These arguments lead us to attribute the slow component in photoconductivity signals to the reduction of the ground state ketone by $TEA_{-H}^{\bullet}$ (reaction 4).

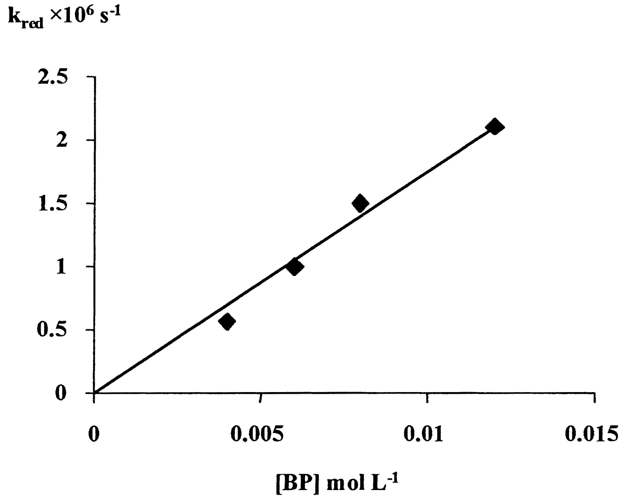

Fig. 8. Plot towards [BP] of the first-order kinetic rate constant k_{red} of the slow component of the photoconductivity signal. Solvent is acetonitrile. Solid line: best linear correlation, leading to a slope of $2 \times 10^8\,M^{-1}\,s^{-1}$ with a correlation coefficient of 0.989.

The quantum yield Φ_{ION} does not show a clear dependence on [BP] or [TEA]. However, a general trend is observed in Table 2: when the ratio [TEA]/[BP] increases, the quantum yield increases also. At constant concentration of BP, this behaviour is comprehensible since an increase

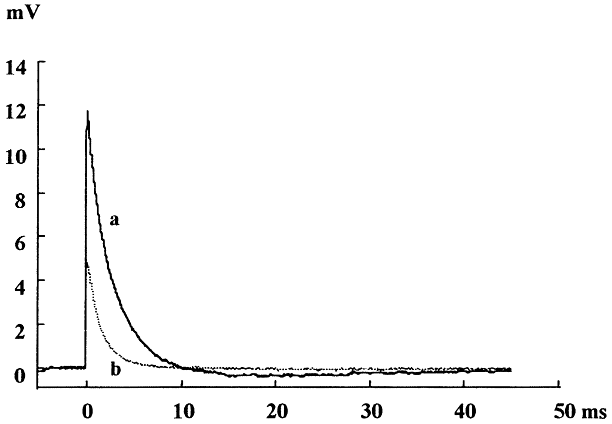

Fig. 9. Effect of adding water on the global photoconductivity signal of an acetonitrile solution of BP 0.012 M, TEA 0.02 M. (a) Addition of 0.05 M of H_2O (b) residual water of commercial acetonitrile.

of [TEA] favours the deprotonation of the ketyl radical. When [TEA] is fixed at 20×10^{-3} M and [BP] is increased, Φ_{ION} decreases. It is quite surprising regarding the fact that increasing [BP] produces more ketyl radicals by Eq. (1), should favour the ions produced by reaction 4 and then should increase Φ_{ION}. The relative quantities of ions produced by secondary reactions are thus very sensitive to working conditions and can not be predicted by simple examination of Eqs. 1–4. It is noteworthy that Φ_{ION} obtained with the addition of 0.05 M of H_2O to ACN is more than twice higher than without H_2O. The role of H_2O is not only to increase slightly k_{red} and k_{dep} but also to produce more ions, as shown in Fig. 9. It is relevant with the NTA experiments and confirms that hydrogen-bondings take an important place within the secondary reactions, regarding that the increase of the relative dielectric constant of ACN is not noticeably changed with the addition of 0.05 M of H_2O. This latter fact was supported by using the same solvent with the reference system BP/DABCO: no significant increase in ion quantum yield was observed. It strongly underlines the sensitivity of dark secondary processes to protic co-solvents. Moreover, Fig. 9 indicates that H_2O changes the kinetic of ion recombination and their lifetime. The recombination kinetic does not follow a clean second order as expected for free ions. An other intriguing aspect is the unusually long lifetime of the ions (millisecond time-scale). Indeed, free ions generally recombine each others in several tens of microseconds. However, the deprotonation of $BPH^{\bullet}$ by TEA produces tertiary alkyl ammonium cations, and it is well known that such ions are rather stable. It must be underlined that in spite of the long lifetime of the ions, they do not have time to migrate towards the electrodes and undergo electrolysis. Assuming that the diffusion coefficient D of each ion is $5 \times 10^{-9}\ \mathrm{m^2\ s^{-1}}$ [30], the ions move approximately from $\Delta l \sim 7\mu m$ during $\Delta t = 5$ ms, as calculated from Eq. (7). This is, thus, too small to monitor an electrical discharge of ions at the electrodes since the laser excitation beam and the platinum plates are separated from about 2 mm.

$$\Delta l = \sqrt{2D\Delta t} \tag{7}$$

The crossing of the baseline and the negative current observed by adding H_2O in ACN (Fig. 9b) generally occur in transient photoconductivity when photoreaction generates species which are able to exchange proton with the solvent [31,32], particularly with residual water [32]. The especially high mobility of hydronium and hydroxide ions changes the offset during the experiment, hence the crossing of the baseline. The intriguing shape of the ion recombination is then possibly due to protonic exchanges between the species formed in reactions 2 and 4 and the residual H_2O. The maximum concentration of this latter in the commercially available ACN we have used is guaranteed under 0.02 M. Even though the concentration should be several times lower, it should stay important towards the amount of excited species formed by the laser beam (ca. around 10^{-5} M). The residual H_2O stays thus in a sufficient concentration to induce secondary reactions in ‘neat’ ACN and to take part within the ion recombination process.

4. Conclusions

The comparative results obtained with NTA and photoconductivity techniques have shown that protic co-solvents play an important role within the dark secondary reactions which follow the photoreduction of BP by TEA. The secondary reduction of BP (reactions 3 and 4) and the ketyl radical deprotonation (reaction 2) are clearly enhanced by protic adducts. Furthermore, the latter reaction can occur with MeOH alone (Eq. (5)). Coupled to the fact that $LiClO_4$ enhances the secondary reduction of BP, the results with H_2O and MeOH lead to the conclusion that dark secondary processes are strongly favoured by increasing the acid-base properties of the solvent, as well as in terms of hydrogen bonding ability than in terms of dative bond exchange between the ketone and a Lewis acid like Li^+. Being aware of this high sensitivity to solvent properties, we have been able to measure the rate constant of Eq. (4) in acetonitrile by using photoconductivity technique and have found $k_{red} = 2 \times 10^8\ \mathrm{M^{-1}\ s^{-1}}$. This high value illustrates the strong reactivity of α-aminoalkyl radicals towards ground state ketones in a polar medium. As the quantum yield of secondary ions depends dramatically on the water concentration (even residual) in acetonitrile, the reactivity of triplet benzophenone towards a tertiary aliphatic amine is by far more intricate than towards aromatic amines or DABCO.

Finally, let us emphasise the two following points. Firstly, photoconductivity, which detects only free ions, appears to be a precious complement to the absorption spectroscopy (by far more frequently used). Photoconductivity offers a good mean to record ion formation kinetics, even when the quantum yield is low, and this sensitivity allows to work at low energy pulse to prevent non linear effects such as photoionisation and triplet–triplet annihilation. The determination of the ion quantum yield is rather simple and does not require the knowledge of the molecular extinction coefficient. For all these reasons, it is surprising that photoconductivity is seldom used to elucidate electron transfer mechanisms. Secondly, the present study offers a supplementary example of the crucial role played by residual water in acetonitrile, a topic which is repeatedly found and disputed in literature.

References

[1] H. Miyasaka, T. Nagata, M. Kiri, N. Mataga, J. Phys. Chem. 96 (1992) 8060.
[2] H. Miyasaka, K. Morita, M. Kiri, N. Mataga, Ultrafast Phenomena VII, Springer, Berlin, 1990, 498.
[3] H. Miyasaka, K. Morita, K. Kamada, N. Mataga, Bull. Chem. Soc. Japan 63 (1990) 3385.
[4] S. Arimitsu, H. Masuhara, N. Mataga, H. Tsubomura, J. Phys. Chem. 79 (1975) 1255.
[5] C. Devadoss, R.W. Fessenden, J. Phys. Chem. 95 (1991) 7253.
[6] J.D. Simon, K.S. Peters, J. Am. Chem. Soc. 103 (1981) 6403.
[7] C.G. Shaeffer, K.S. Peters, J. Am. Chem. Soc. 102 (1980) 7566.
[8] S. Inbar, H. Linschitz, S.G. Cohen, J. Am. Chem. Soc. 103 (1981) 1048.
[9] K. Bhattacharyya, P.K. Das, J. Phys. Chem. 90 (1986) 3987.
[10] S.G. Cohen, H.M. Chao, J. Am. Chem. Soc. 90 (1968) 165.
[11] S.G. Cohen, R.J. Baumgarten, J. Am. Chem. Soc. 87 (1965) 2996.
[12] J.C. Scaiano, J. Phys. Chem. 85 (1981) 2851.
[13] M. von Raumer, A. Sarbach, E. Haselbach, J. Photochem. Photobiol., A: Chem. 121 (1999) 75.
[14] J.-P. Fouassier, A. Erddalane, F. Morlet-Savary, I. Sumiyoshi, M. Harada, M. Kawabata, Macromolecules 27 (1994) 3349.
[15] M. von Raumer, P. Suppan, Chem. Phys. Lett. 250 (1996) 91.
[16] H. Miyasaka, K. Morita, K. Kamada, N. Mataga, Chem. Phys. Lett. 178 (1991) 504.
[17] C. Devadoss, R.W. Fessenden, J. Phys. Chem. 94 (1990) 4540.
[18] K.S. Peters, J. Lee, J. Phys. Chem. 97 (1993) 3761.
[19] R.B. Gupta, J.R. Combes, K.P. Johnston, J. Phys. Chem. 97 (1993) 707.
[20] M. Yamaji, T. Kiyota, H. Shizuka, Chem. Phys. Lett. 226 (1994) 199.
[21] S. Winstein, P.E. Klinedinst Jr., G.C. Robinson, J. Am. Chem. Soc., 83 (1964) 885 and 4986.
[22] A. Loupy, B. Tchoubar, D. Astruc, Chem. Rev. 92 (1992) 1141.
[23] P.A. Thompson, J.D. Simon, J. Am. Chem. Soc. 115 (1993) 5657.
[24] J.D. Simon, K.S. Peters, J. Am. Chem. Soc. 105 (1983) 4875.
[25] J.D. Simon, K.S. Peters, Acc. Chem. Res. 17 (1984) 277.
[26] E. Haselbach, P. Jacques, D. Pilloud, P. Suppan, E. Vauthey, J. Phys. Chem. 95 (1991) 7115.
[27] E. Haselbach, E. Vauthey, P. Suppan, Tetrahedron 44 (1988) 7335.
[28] J.L. Goodman, K.S. Peters, J. Am. Chem. Soc. 108 (1986) 1700.
[29] D. Burget, P. Jacques, E. Vauthey, P. Suppan, E. Haselbach, J. Chem. Soc. Faraday Trans. 90 (1994) 2481.
[30] P. Jacques, X. Allonas, Chem. Phys. Lett. 233 (1995) 533.
[31] F. Elisei, G. Favaro, H. Görner, J. Photochem. Photobiol., A: Chem. 59 (1991) 243.
[32] S.G. Ballard, D.C. Mauzerall, G. Tollin, J. Phys. Chem. 80 (1976) 341.